The Physics of Permanent-Magnet "Motors"

L. David Roper
Department of Physics
Virginia Polytechnic Institute and State University
Blacksburg, Virginia 24061

Abstract

We derive equations for the potential energy of a linear permanent-magnet "motor" in several magnetic configurations of increasing complexity, and plot the equations for representative sets of parameters. This clearly shows the relationship between magnetic configuration complexity and uniformity of acceleration. Such a linear permanent-magnet device is somewhat equivalent to a catapult, or a slingshot, or a piledriver.

I. Introduction

A recent United States patent (1) is for "permanent-magnet motors." Two types of "motors" are described in the patent, one linear and one circular. We shall discuss in this paper the physics of the linear device, which will then enable us to show that the circular "motor" cannot sustain continuous motion without input of external mechanical energy. The linear "motor" is somewhat equivalent to a catapult, a slingshot, or a piledriver, whose basic thrusting effect can be achieved by a much simpler magnet arrangement than described in the patent.

II. Linear Device Configuration.

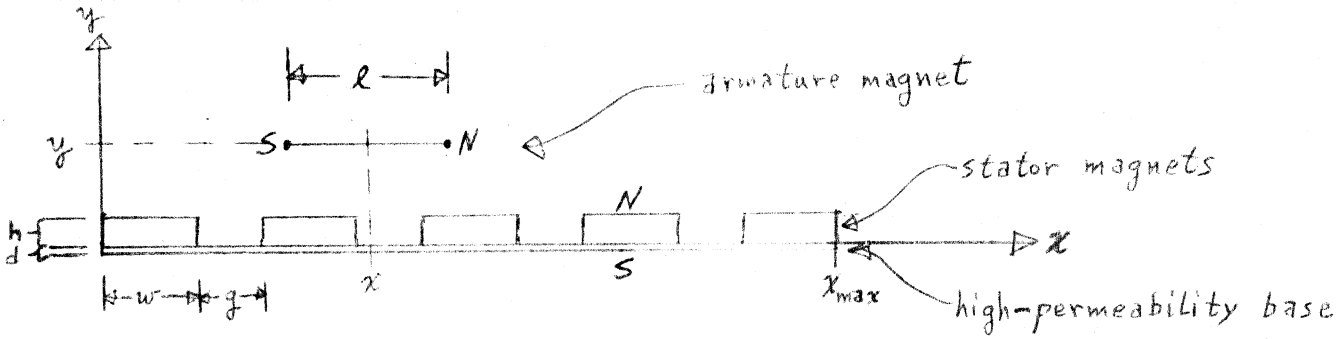

Figure 1. Configuration of linear permanent-magnet motor. The stator magnets are bonded to the high-permeability base. The armature magnet is constrained to move parallel to the stator magnets.

Figure 1 shows the configuration of the linear permanent-magnet device. The high-permeability base material affects the magnetic fields in a way we shall discuss later. However, the basic effect of the linear device can be achieved with a much simpler magnetic

arrangement, which is shown in Fisure 2.

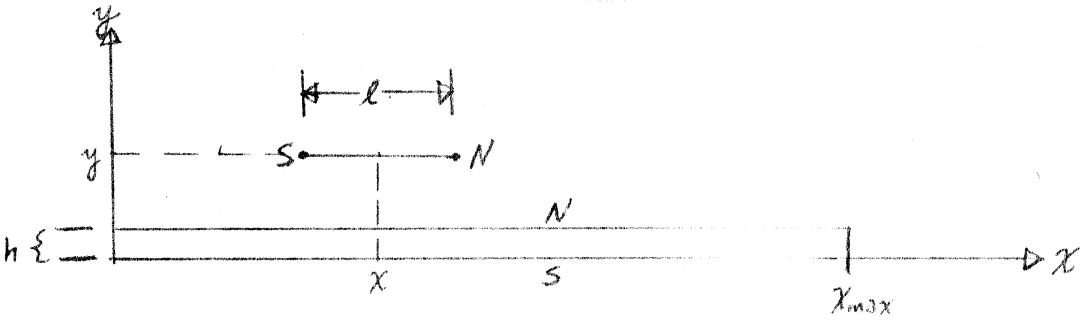

Figure 2. Simplest arrangement for a linear permanent-magnet motor.

III. Analysis of The Simple Linear Permanent-Magnet Device

Without loss of generality we can consider only two dimensions as shown in Fisure 2 and consider the north and south poles of the stator magnet to be lines of uniform magnetic poles of density $\rho_s = m_s / x_{max}$,

where m_s is the total pole strength of the stator magnet. The potential energy of an armature pole of strength m_a at position (x,y) relative to and due to the stator line of poles is derived as follows:

$$V(x) = m_a \rho_s \int_0^{x_{max}} \frac{dx'}{\sqrt{(x'-x)^2 + y^2}} = m_a \rho_s \ln\left(\frac{x_{max} - x + \sqrt{(x_{max}-x)^2 + y^2}}{-x + \sqrt{x^2 + y^2}} \right) \quad (1)$$

Applying Equation (1) to both armature poles interacting with both stator lines of poles in Fisure 2, we get:

$V(x) = V_N(x) + V_S(x)$ (The indices N and S refer to the armature poles.),

where $V_N(x) = V_{NN}(x) + V_{NS}(x)$, $V_S(x) = V_{SN}(x) + V_{SS}(x)$,

$$V_{NN}(x) = m_a \rho_s \ln\left(\frac{x_{max} - x - \frac{\ell}{2} + \sqrt{(x_{max} - x - \frac{\ell}{2})^2 + (y-h)^2}}{-x - \frac{\ell}{2} + \sqrt{(x+\frac{\ell}{2})^2 + (y-h)^2}} \right),$$

$$V_{NS}(x) = -m_a \rho_s \ln\left(\frac{x_{max} - x - \frac{\ell}{2} + \sqrt{(x_{max} - x - \frac{\ell}{2})^2 + y^2}}{-x - \frac{\ell}{2} + \sqrt{(x+\frac{\ell}{2})^2 + y^2}} \right), \quad (2)$$

$$V_{SN}(x) = -m_a \rho_s \ln\left(\frac{x_{max} - x + \frac{\ell}{2} + \sqrt{(x_{max} - x + \frac{\ell}{2})^2 + (y-h)^2}}{-x + \frac{\ell}{2} + \sqrt{(x-\frac{\ell}{2})^2 + (y-h)^2}} \right), \text{ and}$$

$$V_{SS}(x) = m_a \rho_s \ln\left(\frac{x_{max} - x + \frac{\ell}{2} + \sqrt{(x_{max} - x + \frac{\ell}{2})^2 + y^2}}{-x + \frac{\ell}{2} + \sqrt{(x-\frac{\ell}{2})^2 + y^2}} \right).$$

The index of the singly indexed energy terms and the first index of the doubly indexed energy terms refers to the pole types of the armature magnet. The second index of the doubly indexed energy terms refers to the pole types of the stator magnet.

Combining these equations, one gets:

$$V(x) = Ma\beta s \ln\left[\left(\frac{x_{max}-x-\frac{\ell}{2}+\sqrt{(x_{max}-x-\frac{\ell}{2})^2+(y-h)^2}}{-x-\frac{\ell}{2}+\sqrt{(x+\frac{\ell}{2})^2+(y-h)^2}}\right)\cdot\left(\frac{x-\frac{\ell}{2}+\sqrt{(x+\frac{\ell}{2})^2+y^2}}{x_{max}-x-\frac{\ell}{2}+\sqrt{(x_{max}-x-\frac{\ell}{2})^2+y^2}}\right)\cdot\left(\frac{-x+\frac{\ell}{2}+\sqrt{(x-\frac{\ell}{2})^2+(y-h)^2}}{x_{max}-x+\frac{\ell}{2}+\sqrt{(x_{max}-x+\frac{\ell}{2})^2+(y-h)^2}}\right)\cdot\left(\frac{x_{max}-x+\frac{\ell}{2}+\sqrt{(x_{max}-x+\frac{\ell}{2})^2+y^2}}{-x+\frac{\ell}{2}+\sqrt{(x-\frac{\ell}{2})^2+y^2}}\right)\right] \quad (3)$$

Equation 3 is plotted in Figure 3 for a representative set of values of the parameters h, y, and l. (See Figure 2.)

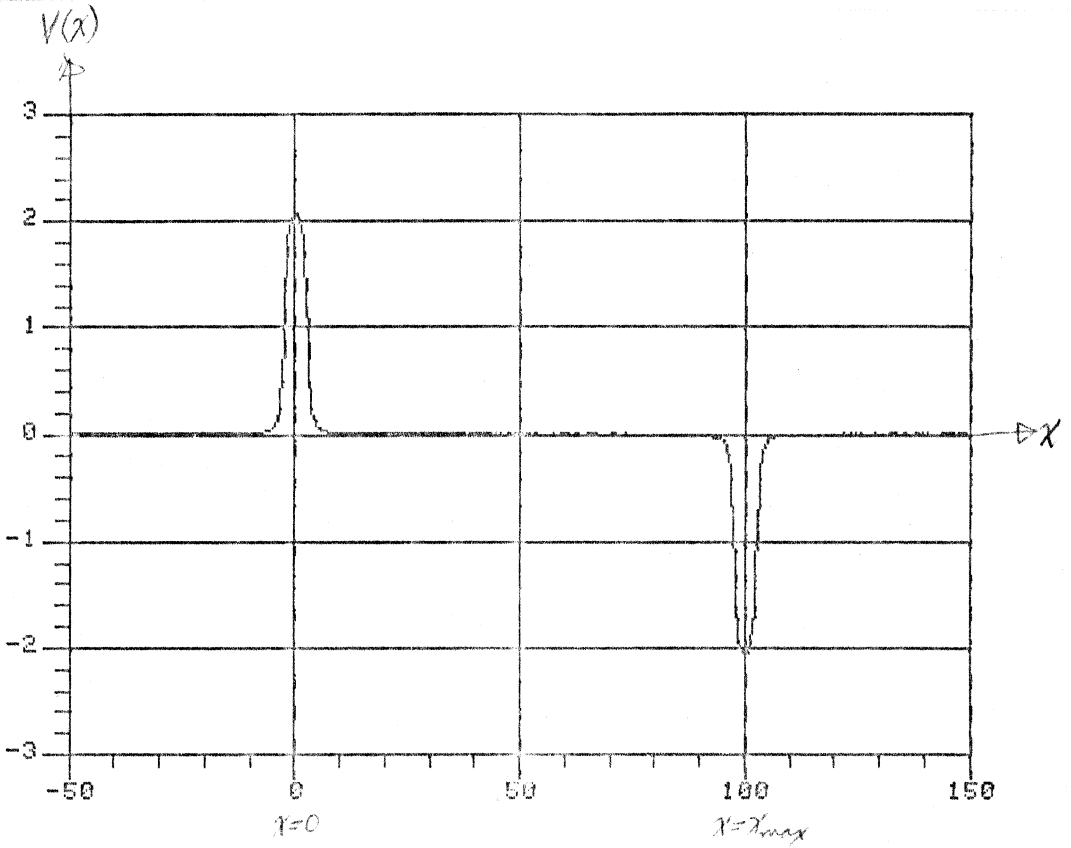

Figure 3. Potential energy versus distance for the configuration of Figure 2.
$(x_{max}/h = 100,\ \ell/h = 5,\ (y-h)/h = 0.5)$

Note in Figure 3 that, if one initially places the armature magnet a small distance to the right of x=0, the magnet will accelerate to the right for a short distance, then coast to near x=xmax, then accelerate to x=xmax, then decelerate a short distance past x=xmax, and then coast on forever if no friction were present. A target placed at x=xmax would receive the full brunt of the magnetic potential energy converted to kinetic energy of the armature magnet. (Perhaps there is some useful purpose for this linear magnetic "motor" but we do not address that possibility here. It could be called a "magnetic catapult", "magnetic slingshot", or "magnetic piledriver.")

If the armature magnet is initially placed at x=xmax, it will require applied work to remove it from there. If it is placed a small distance to the left of x=0, it will accelerate to the left a short distance, and then coast forever if there were no friction. (Starting it slightly to the right of x=0 with a target at x=xmax would be the ideal setup for a "piledriver"; whereas, the "slingshot" or "catapult" for long distance movement would work equally well by starting the armature magnet on either side of x=0.)

IV. Analysis of a Linear Magnetic Device with a Segmented Stator Magnet

Figure 2 can be easily changed to be more nearly like Figure 1 by segmenting the stator magnet as shown in Figure 4.

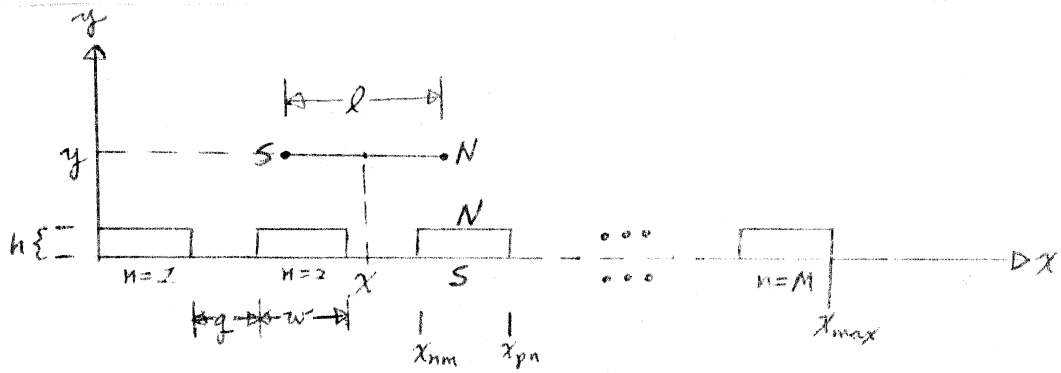

Figure 4. Segmentation of stator magnet in Figure 2 into several stator magnets.

The potential energy components for Figure 3 are (see Equations 2):

$$V(x) = V_{NN}(x) + V_{NS}(x) + V_{SN}(x) + V_{SS}(x) \text{ ; where}$$

$$V_{NN}(x) = m_a \rho_s \sum_{n=1}^{M} \ln\left(\frac{x_{np} - x - \frac{\ell}{2} + \sqrt{(x_{np} - x - \frac{\ell}{2})^2 + (y-h)^2}}{x_{nm} - x - \frac{\ell}{2} + \sqrt{(x_{nm} - x - \frac{\ell}{2})^2 + (y-h)^2}} \right),$$

$$V_{NS}(x) = -m_a \rho_s \sum_{n=1}^{M} \ln\left(\frac{x_{np} - x - \frac{\ell}{2} + \sqrt{(x_{np} - x - \frac{\ell}{2})^2 + y^2}}{x_{nm} - x - \frac{\ell}{2} + \sqrt{(x_{nm} - x - \frac{\ell}{2})^2 + y^2}} \right), \quad (4)$$

$$V_{SN}(x) = -m_a \rho_s \sum_{n=1}^{M} \ln\left(\frac{x_{np} - x + \frac{\ell}{2} + \sqrt{(x_{np} - x + \frac{\ell}{2})^2 + (y-h)^2}}{x_{nm} - x + \frac{\ell}{2} + \sqrt{(x_{nm} - x + \frac{\ell}{2})^2 + (y-h)^2}} \right), \text{ and}$$

$$V_{SS}(x) = m_a \rho_s \sum_{n=1}^{M} \ln\left(\frac{x_{np} - x + \frac{\ell}{2} + \sqrt{(x_{np} - x + \frac{\ell}{2})^2 + y^2}}{x_{nm} - x + \frac{\ell}{2} + \sqrt{(x_{nm} - x + \frac{\ell}{2})^2 + y^2}} \right), \text{ where}$$

$x_{nm} \equiv (n-1)(g+w)$ and $x_{np} \equiv x_{nm} + w = (n-1)g + nw$.

The sum of all of the potential energy components given in Equation (4) are plotted in Fisure 5 for a representative set of values of the parameters h, y, l, w, and s. (See Fisure 4.) The main difference between this fisure and Figure 3 is the presence of oscillations in the formerly flat resion between the magnet "hill" and "valley".

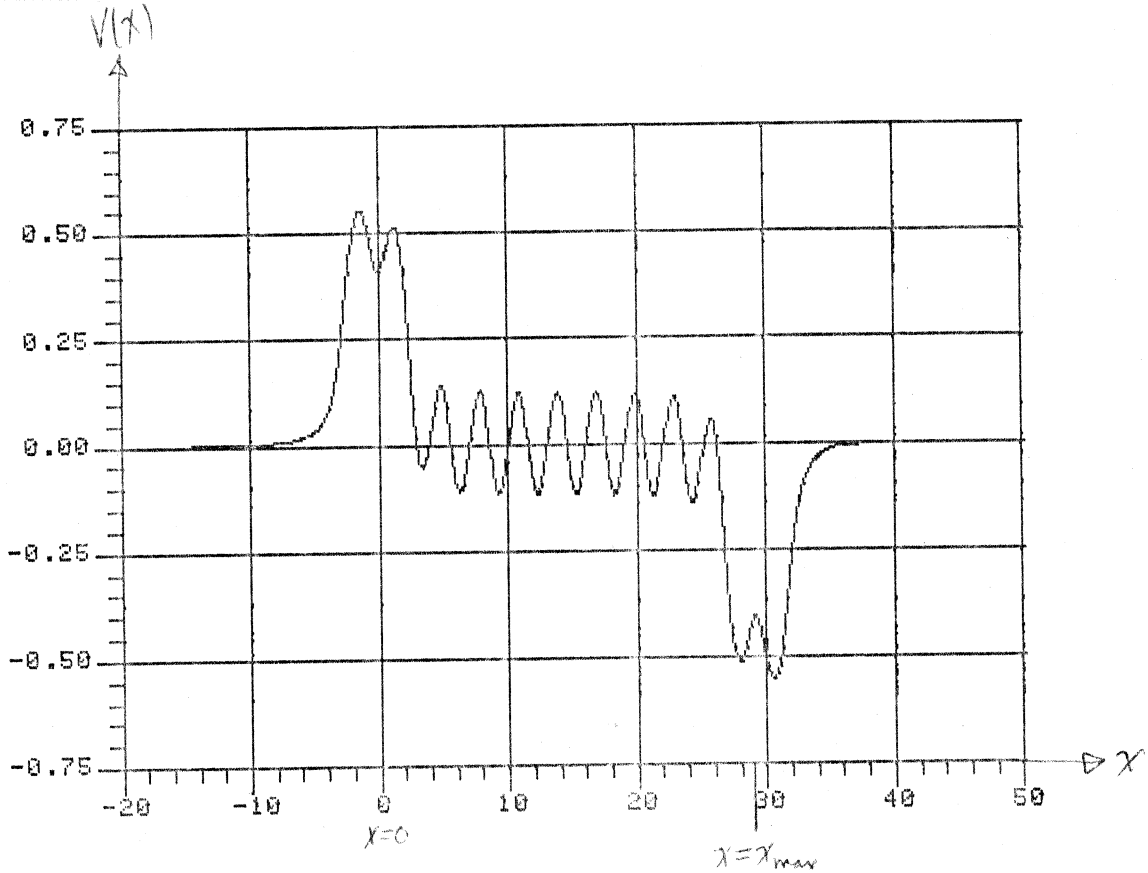

Figure 5. Potential energy versus distance for the configuration of Figure 4.

{M=10, w/g=2, [ℓ-(2w+g)]/g=0.2, h/g=0.5, (y-h)/g=1}

V. Analysis of a Linear Device with a Segmented Stator Magnet on a High-Permeability Base

It is not easy to precisely determine how the magnetic south poles of the stator magnet are distributed when the magnets are placed on a high-permeability base. The base is a voracious consumer of magnetic lines of force. We consider two extreme cases that are easy to calculate. The actual case would lie between the two extremes. One unlikely extreme assumption for the magnetic field lines for this confisuration (Figure 1) is represented in Fisure 6. As shown, the magnetic field lines are assumed to bunch tosether as they enter the base from below. Also, the pole linear density of the topside stator south poles is assumed to be the same as the stator north poles' linear density.

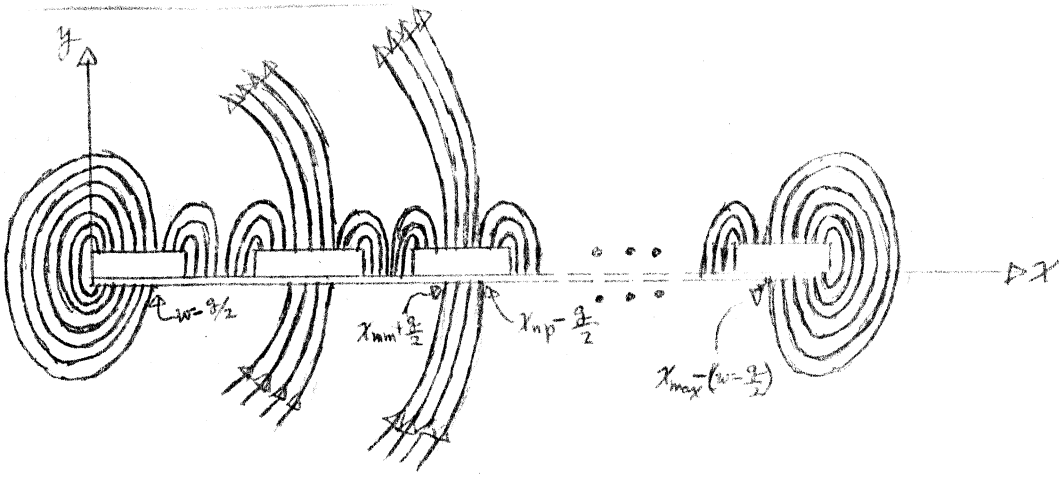

Figure 6a. Idealized magnetic field lines for the stator arrangement of Figure 1. ($w/g > 1$) (See Figure 1 for labels.)

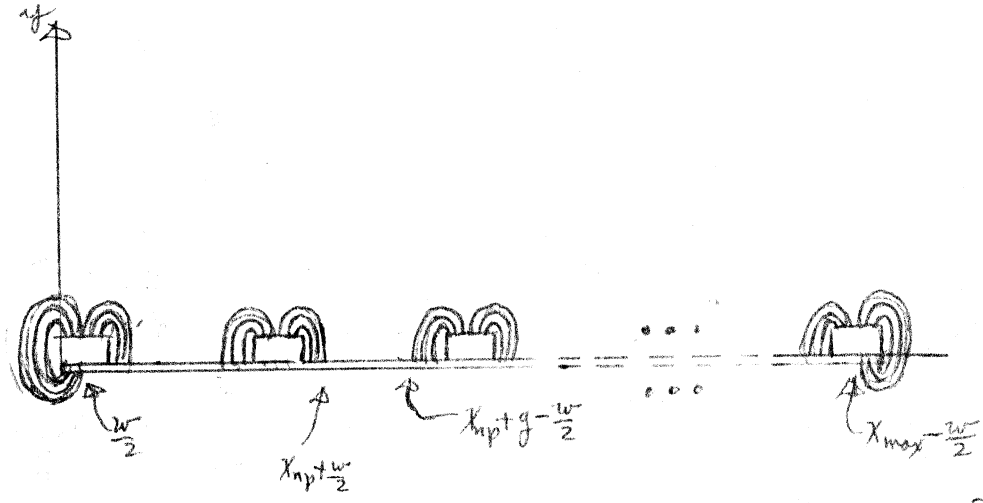

Figure 6b. Idealized magnetic field lines for the stator arrangement of Figure 1. ($w/g < 1$) (See Figure 1 for labels.)

As shown in Fisure 6, the stator poles are located differently depending on the ratio of w/s. For w/s<1 the potential energy components are:

$$V(x) = V_{NN}(x) + V_{NS}(x) + V_{SN}(x) + V_{SS}(x), \text{ where}$$

$V_{NN}(x)$ = same as in Equation (4), $V_{SN}(x)$ = same as in Equation (4),

$$V_{NS}(x) = -Ma\rho_s \sum_{n=2}^{M-1} \ln\left[\left(\frac{x_{np}+\frac{w}{2}-x-\frac{\ell}{2}+\sqrt{(x_{np}+\frac{w}{2}-x-\frac{\ell}{2})^2+y^2}}{x_{np}-x-\frac{\ell}{2}+\sqrt{(x_{np}-x-\frac{\ell}{2})^2+y^2}}\right)\cdot\left(\frac{x_{np}+g-x-\frac{\ell}{2}+\sqrt{(x_{np}+g-x-\frac{\ell}{2})^2+y^2}}{x_{np}+g-\frac{w}{2}-x-\frac{\ell}{2}+\sqrt{(x_{np}+g-\frac{w}{2}-x-\frac{\ell}{2})^2+y^2}}\right)\right]$$

$$-Ma\rho_s \ln\left[\left(\frac{\frac{w}{2}-x-\frac{\ell}{2}+\sqrt{(\frac{w}{2}-x-\frac{\ell}{2})^2+(y+d)^2}}{-x-\frac{\ell}{2}+\sqrt{(x+\frac{\ell}{2})^2+(y+d)^2}}\right)\cdot\left(\frac{x_{max}-x-\frac{\ell}{2}+\sqrt{(x_{max}-x-\frac{\ell}{2})^2+(y+d)^2}}{x_{max}-\frac{w}{2}-x-\frac{\ell}{2}+\sqrt{(x_{max}-\frac{w}{2}-x-\frac{\ell}{2})^2+(y+d)^2}}\right)\right], \quad (5)$$

and

$$V_{SS}(x) = Ma\rho_s \sum_{n=2}^{M-2} \ln\left[\left(\frac{x_{np}+\frac{w}{2}-x+\frac{\ell}{2}+\sqrt{(x_{np}+\frac{w}{2}-x+\frac{\ell}{2})^2+y^2}}{x_{np}-x+\frac{\ell}{2}+\sqrt{(x_{np}-x+\frac{\ell}{2})^2+y^2}}\right)\cdot\left(\frac{x_{np}+g-x+\frac{\ell}{2}+\sqrt{(x_{np}+g-x+\frac{\ell}{2})^2+y^2}}{x_{np}+g-\frac{w}{2}-x+\frac{\ell}{2}+\sqrt{(x_{np}+g-\frac{w}{2}-x+\frac{\ell}{2})^2+(y+d)^2}}\right)\right]$$

$$+Ma\rho_s \ln\left[\left(\frac{\frac{w}{2}-x+\frac{\ell}{2}+\sqrt{(\frac{w}{2}-x+\frac{\ell}{2})^2+(y+d)^2}}{-x+\frac{\ell}{2}+\sqrt{(x-\frac{\ell}{2})^2+(y+d)^2}}\right)\cdot\left(\frac{x_{max}-x+\frac{\ell}{2}+\sqrt{(x_{max}-x+\frac{\ell}{2})^2+(y+d)^2}}{x_{max}-\frac{w}{2}-x+\frac{\ell}{2}+\sqrt{(x_{max}-\frac{w}{2}-x+\frac{\ell}{2})^2+(y+d)^2}}\right)\right],$$

where $x_{nm} \equiv (n-1)(g+w)$ and $x_{np} = x_{nm} + w$.

For w/s>1, $V_{NN}(x)$ and $V_{SN}(x)$ are the same as for w/s<1 given above, but

$$V_{NS}(x) = -Ma\rho_s \sum_{n=1}^{M-1} \ln\left[\left(\frac{x_{np}+g-x-\frac{\ell}{2}+\sqrt{(x_{np}+g-x-\frac{\ell}{2})^2+y^2}}{x_{np}-x-\frac{\ell}{2}+\sqrt{(x_{np}-x-\frac{\ell}{2})^2+y^2}}\right)\cdot\left(\frac{x_{np}-\frac{g}{2}-x-\frac{\ell}{2}+\sqrt{(x_{np}-\frac{g}{2}-x-\frac{\ell}{2})^2+(y+d)^2}}{x_{nm}+\frac{g}{2}-x-\frac{\ell}{2}+\sqrt{(x_{nm}+\frac{g}{2}-x-\frac{\ell}{2})^2+(y+d)^2}}\right)\right]$$

$$-Ma\rho_s \ln\left[\left(\frac{w-\frac{g}{2}-x-\frac{\ell}{2}+\sqrt{(w-\frac{g}{2}-x-\frac{\ell}{2})^2+(y+d)^2}}{-x-\frac{\ell}{2}+\sqrt{(x+\frac{\ell}{2})^2+(y+d)^2}}\right)\cdot\left(\frac{x_{max}-x-\frac{\ell}{2}+\sqrt{(x_{max}-x-\frac{\ell}{2})^2+(y+d)^2}}{x_{max}-w+\frac{g}{2}-x-\frac{\ell}{2}+\sqrt{(x_{max}-w+\frac{g}{2}-x-\frac{\ell}{2})^2+(y+d)^2}}\right)\right], \quad (6)$$

and

$$V_{SS}(x) = Ma\rho_s \sum_{n=1}^{M} \ln\left[\left(\frac{x_{np}+g-x+\frac{\ell}{2}+\sqrt{(x_{np}+g-x+\frac{\ell}{2})^2+y^2}}{x_{np}-x+\frac{\ell}{2}+\sqrt{(x_{np}-x+\frac{\ell}{2})^2+y^2}}\right)\cdot\left(\frac{x_{np}-\frac{g}{2}-x+\frac{\ell}{2}+\sqrt{(x_{np}-\frac{g}{2}-x+\frac{\ell}{2})^2+(y+d)^2}}{x_{nm}+\frac{g}{2}-x+\frac{\ell}{2}+\sqrt{(x_{nm}+\frac{g}{2}-x+\frac{\ell}{2})^2+(y+d)^2}}\right)\right]$$

$$+Ma\rho_s \ln\left[\left(\frac{w-\frac{g}{2}-x+\frac{\ell}{2}+\sqrt{(w-\frac{g}{2}-x+\frac{\ell}{2})^2+(y+d)^2}}{-x+\frac{\ell}{2}+\sqrt{(x-\frac{\ell}{2})^2+(y+d)^2}}\right)\cdot\left(\frac{x_{max}-x+\frac{\ell}{2}+\sqrt{(x_{max}-x+\frac{\ell}{2})^2+(y+d)^2}}{x_{max}-w+\frac{g}{2}-x+\frac{\ell}{2}+\sqrt{(x_{max}-w+\frac{g}{2}-x+\frac{\ell}{2})^2+(y+d)^2}}\right)\right].$$

Equations (6) are plotted in Figure 7 for a representative set of values of the parameters h, g, l, w, s, and d.

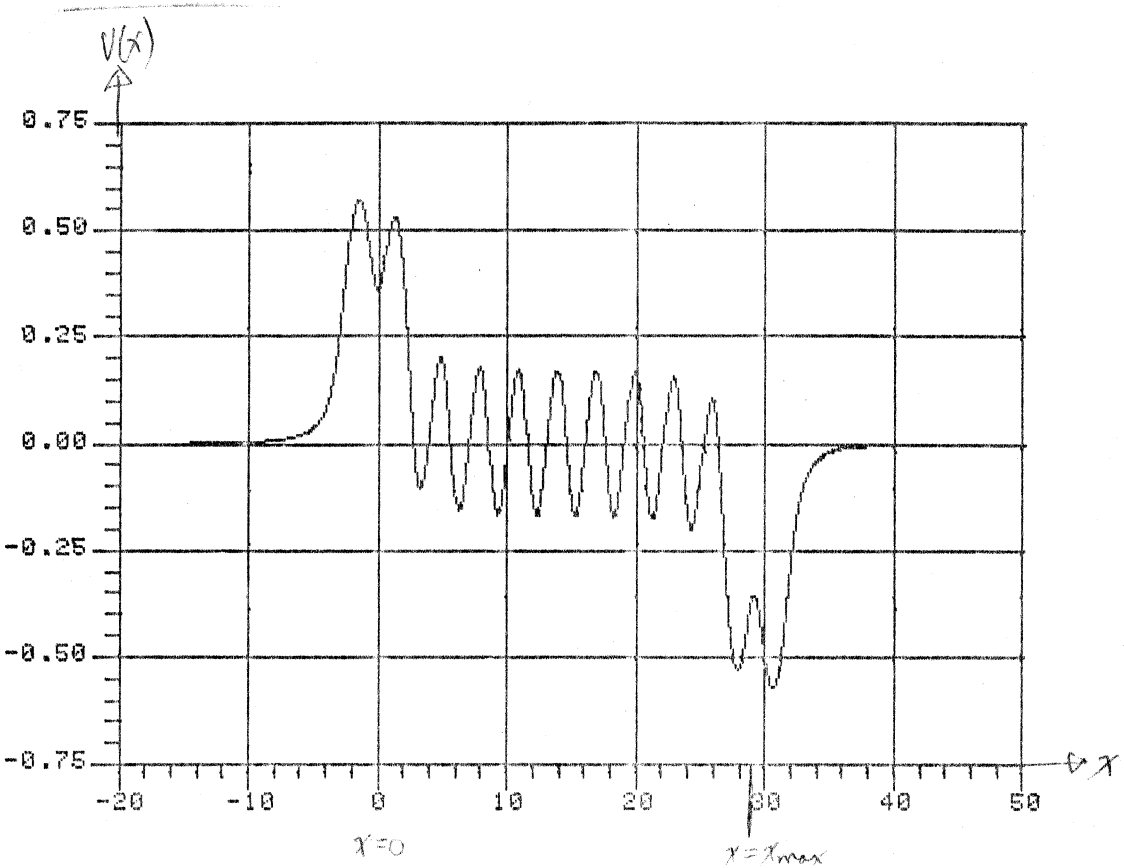

Figure 7. Potential energy versus distance for the configuration of Figure 6a.

$\{M=10,\ w/g=2,\ [e-(2w+g)]/g=0.2,\ h/g=0.5,\ (y-h)/g=1\}$

The opposite unlikely extreme assumption for the magnetic field lines for the Figure 1 configuration is represented in Figure 8. Here the magnetic field lines are assumed to be distributed evenly, except at the edges, as they enter the base from below.

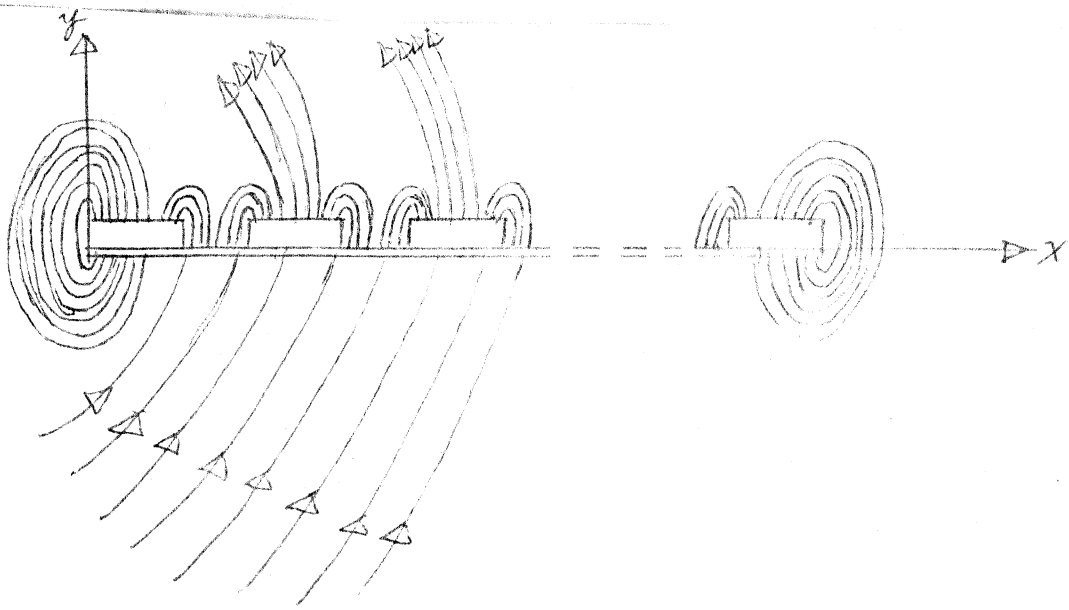

Figure 8. Idealized magnetic field lines for the stator arrangement of Figure 1. ($w/g > 1$)
For $w/g < 1$, see Figure 6b.
(See Figures 1 and 6a for labels.)

For w/s<1 the potential energy components remain as for Figure 6 given in Equation (5). For w/s>1 the potential energy components are:

$$V(x) = V_{NN}(x) + V_{NS}(x) + V_{SN}(x) + V_{SS}(x)\ , \text{ where}$$

$V_{NN}(x)$ = same as in Equation (4), $V_{SN}(x)$ = same as in Equation (4),

$$V_{NS}(x) = -M a f_s f \ln\left(\frac{x_{max} - \frac{w}{2} - x - \frac{\ell}{2} + \sqrt{(x_{max} - \frac{2w}{2} - x - \frac{\ell}{2})^2 + (y+d)^2}}{\frac{w}{2} - x - \frac{\ell}{2} + \sqrt{(\frac{2w}{2} - x - \frac{\ell}{2})^2 + (y+d)^2}}\right)$$

$$- M a f_s \ln\left[\left(\frac{\frac{w}{2} - x - \frac{\ell}{2} + \sqrt{(\frac{2w}{2} - x - \frac{\ell}{2})^2 + (y+d)^2}}{-x - \frac{\ell}{2} + \sqrt{(x+\frac{\ell}{2})^2 + (y+d)^2}}\right) \cdot \left(\frac{x_{max} - x - \frac{\ell}{2} + \sqrt{(x_{max} - x - \frac{\ell}{2})^2 + (y+d)^2}}{x_{max} - \frac{w}{2} - x - \frac{\ell}{2} + \sqrt{(x_{max} - \frac{2w}{2} - x - \frac{\ell}{2})^2 + (y+d)^2}}\right)\right], \quad \text{and}$$

$$V_{SS}(x) = M a f_s f \ln\left(\frac{x_{max} - \frac{w}{2} - x + \frac{\ell}{2} + \sqrt{(x_{max} - \frac{w}{2} - x + \frac{\ell}{2})^2 + (y+d)^2}}{\frac{w}{2} - x + \frac{\ell}{2} + \sqrt{(\frac{w}{2} - x + \frac{\ell}{2})^2 + (y+d)^2}}\right) \qquad (7)$$

$$+ M a f_s \ln\left[\left(\frac{\frac{w}{2} - x + \frac{\ell}{2} + \sqrt{(\frac{w}{2} - x + \frac{\ell}{2})^2 + (y+d)^2}}{-x + \frac{\ell}{2} + \sqrt{(x - \frac{\ell}{2})^2 + (y+d)^2}}\right) \cdot \left(\frac{x_{max} - x + \frac{\ell}{2} + \sqrt{(x_{max} - x + \frac{\ell}{2})^2 + (y+d)^2}}{x_{max} - \frac{w}{2} - x + \frac{\ell}{2} + \sqrt{(x_{max} - \frac{w}{2} - x + \frac{\ell}{2})^2 + (y+d)^2}}\right)\right], \text{ where}$$

$f \equiv [Mw - (M-1)g - 2(w-1)]/[x_{max} - 2(w-1)]$ is the appropriate area ratio to give equal north and south stator poles.

Equations (7) are plotted in Figure 9 for a representative set of values of the parameters h, g, l, w, s, and d.

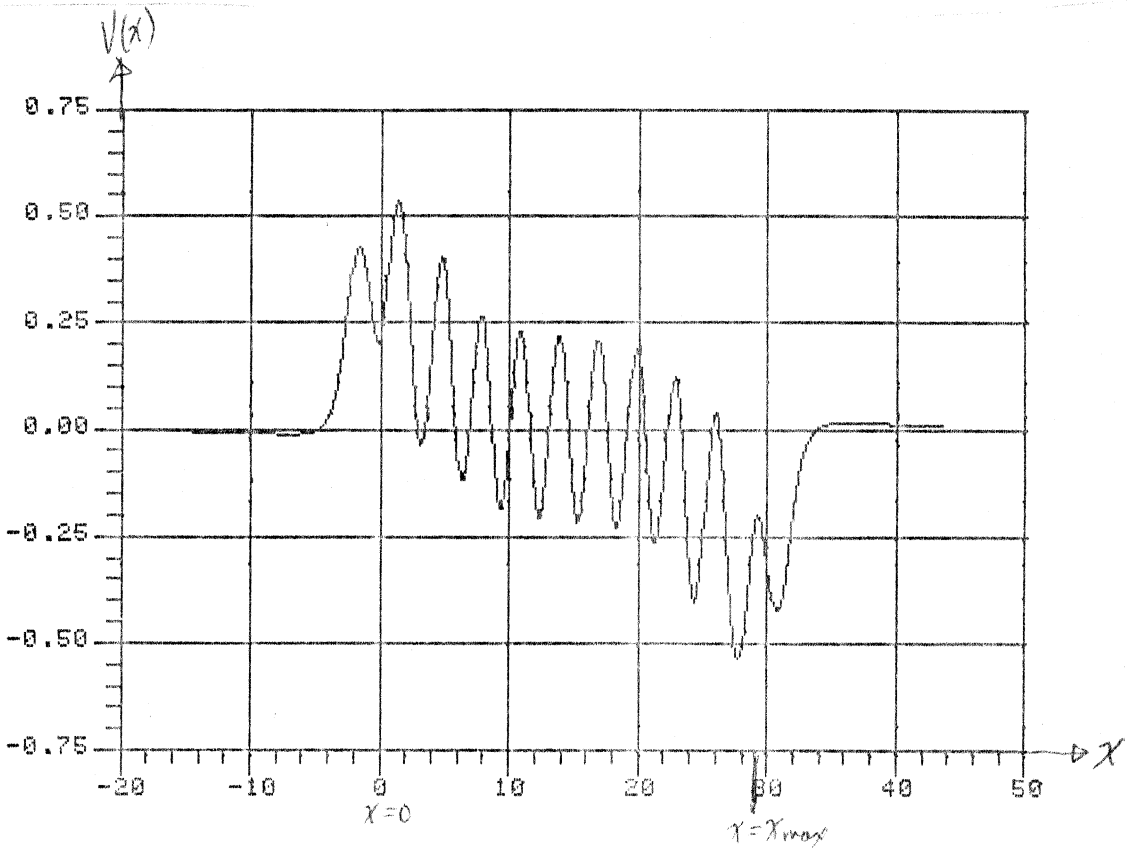

Figure 9. Potential energy versus distance for the configuration of Figure 8,

$\{M=10,\ w/g=2,\ [e-(2w+g)]/g=0.2,\ h/g=0.5,\ (y-h)/g=1\}$

The actual situation probably lies somewhere between Figure 7 and Figure 9. Note that, in addition to the hill and well at the two ends and the oscillations in between, that were present for the simpler configurations discussed above, there is also a gradual decline from the hill to the well that was not previously present.

VI. Multiple-Magnet Armatures

The oscillatory nature of the gradually decreasing area between the hill and the well of Figure 9 can be smoothed out, as indicated in the patent (1), by staggering several armature magnets attached together, as shown in Figure 10.

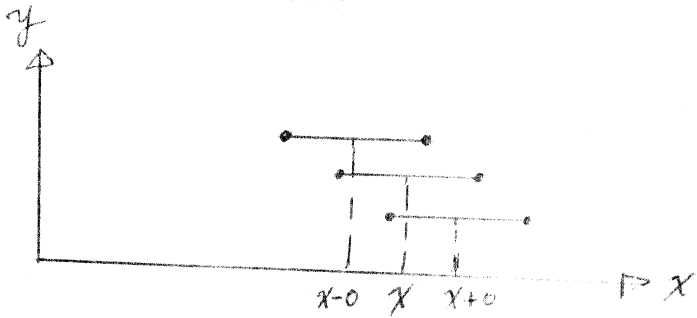

Figure 10. Three armature magnets offset from each other by a distance o in the x direction. There is no offset in the y direction; they are shown offset in y for clarity. Of course, they are offset in the z direction (into the paper), but that has no effect on their motion.

Figures 11 and 12 show how Figures 7 and 9 are changed when an offset of 1.5 (in units of gap width, g) is selected. The actual situation of Figure 1 will yield a potential energy curve behaviour somewhere between that of Figure 7 and Figure 9.

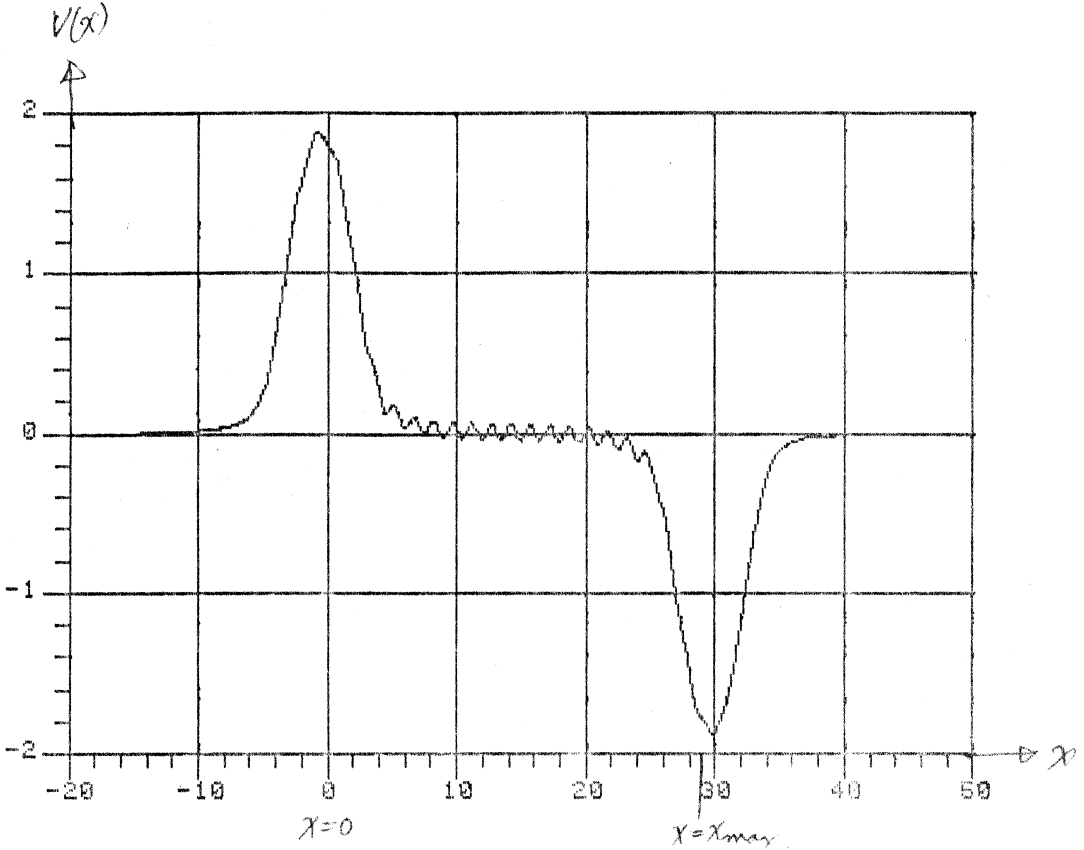

Figure 11. Potential energy versus distance for the configuration of Figure 6a with three offset armature magnets (see Figure 10).

$\{M=10,\ w/g=2,\ [\ell-(2w+g)]/g=0.2,\ h/g=0.5,\ (y-h)/g=1,\ o/g=1.5\}$

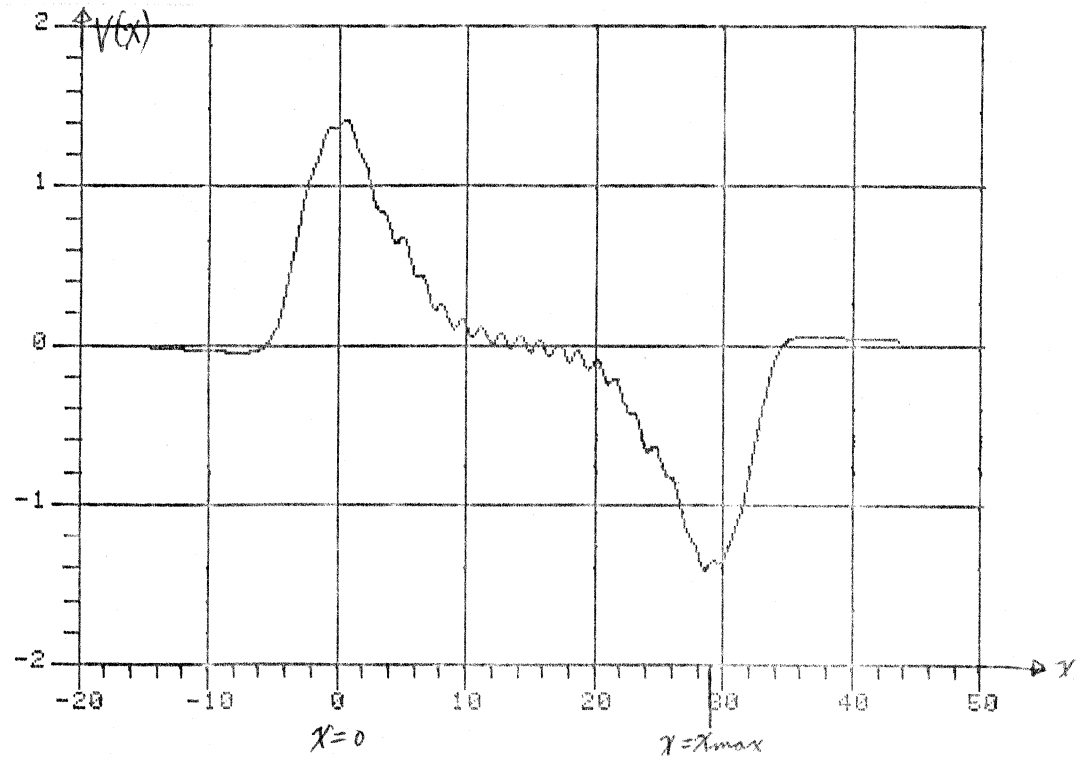

Figure 12. Potential energy versus distance for the configuration of Figure 8 with three offset armature magnets (see Figure 10),

$\{M=10,\ w/g=2,\ [\ell-(2w+g)]/g=0.2,\ h/g=0.5,\ (y-h)/g=1,\ o=1.5\}$

VII. Conclusions

The main effect of a linear permanent-magnet "motor" of the type described herein is present in the simplest type depicted in Figure 2. Its potential energy curves are shown in Figure 3. If the armature magnet is placed on the "magnet hill" by expenditure of mechanical energy, some of that mechanical energy will be regenerated when the magnet "slides down" the hill. The device could be used as a power magnifier. That is, a relatively long time could be used to convert mechanical energy into the magnetic potential energy at the "hill" position; then a relatively short time would elapse in "sliding down" the hill.

Adding complexities to Figure 2 to make it more like Figure 1 and offsetting several armature magnets cause a gradual potential energy slope (Figures 11 and 12) between the "magnetic hill" and the "magnetic valley", rather than the flat area of Figure 3.

Finally, putting several linear devices in a circle accomplishes nothing more than creating several oscillators in a circle. Releasing an armature magnet constrained to move on a circle concentric with the stator's circle, will result in decaying oscillatory motion.

Putting two linear devices in line creates a non-harmonic mechanical

oscillator, and it can be made either symmetric or nonsymmetric.

VIII. Acknowledgements

The author was allowed by the inventor, Mr. Howard Johnson, to examine the actual devices and thereby ascertained that the devices behaved very closely to the results derived above. The author wishes to thank Mr. Johnson for the opportunity to examine the devices.

The author also wishes to thank Dr. Brian Dennison for several ideas related to this work.

IX. References

1. United States Patent No. 4,151,431